

## The axisymmetric computational study of a femoral component to analysis the effect of titanium alloy and diameter variation

Ana Rita Carreiras <sup>a</sup>, Elza M. M. Fonseca <sup>b, \*</sup>, Diana Martins <sup>c</sup> and Rui Couto <sup>c</sup>

<sup>a</sup> Engenharia Mecânica, ISEP | Instituto Superior de Engenharia do Porto, Porto, Portugal

<sup>b</sup> LAETA, INEGI, Engenharia Mecânica, ISEP | Instituto Superior de Engenharia do Porto, Porto, Portugal

<sup>c</sup> Engenharia Mecânica, ISEP, Instituto Superior de Engenharia do Porto, Porto, Portugal

### ARTICLE INFO

#### Article history:

Received: 13 July 2020

Accepted: 19 August 2020

#### Keywords:

Stiffness

Bone

Numerical model

Load transferred to the bone

### ABSTRACT

This work presents a numerical approach in order to predict the influence of implant material stiffness in a femoral component design when submitted in compression. The implant success depends on the transferred load to the neighboring bone. The finite element method can be used to analysis the stress and strain distribution in the femoral component allowing to improve the implant selection. For this purpose, 2D axisymmetric computational models of an implant-cement-bone (Model 1), implant-bone (Model 2) and core implant-bone (Model 3) were constructed using the finite element method with ANSYS program. The finite element model was assumed a state of ideal osseointegration, where the cortical bone, cement and implant were assumed as perfectly bonded. Three different implant diameters were chosen and two materials considered, a typical titanium alloy and iso-elastic titanium alloy with low stiffness. The finite element analysis was carried out to calculate the von Mises stress, the shear stress and the strain energy density in all studied models. Also, an analytical procedure, based on the elastic stress theory and applied to composite materials for an axial load, was used to measure the load transferred to the bone. In all results, Model 3 with the vertical graded iso-elastic alloy in vicinity to the bone with high diameter has a good performance.

### 1. Introduction

In orthopedic, osseointegration is described to be affect by many reasons, implant design, surface treatment, bone quality, surgical technique, post-operative care.<sup>1</sup> According different investigations the less stiff implant to improve fracture healing and prevent bone weakening due to stress shielding.<sup>2</sup> But, it is not totally exact to say that bone implant with high stiffness causes excessive stress shielding, because beyond the stiffness that is characterized by the material property, the cross-section geometry has an influence in conjunction.<sup>2</sup> According the imposed mechanical loads, stresses and strains can induce morphological changes and bone weakening for a revision implant, particularly with the use of uncemented implants.<sup>3</sup>

The implant material and dimension are one of the dominant problems and affect the developed stress levels into the bone resorption.<sup>1,4</sup> Femoral implant is made using materials such as metals, ceramics, polymers and composites.<sup>5</sup> Metallic biomaterials are important and used to improve the patient quality life. Moreover, the bio functionality of these materials needs to be improved<sup>6</sup> in order to create new materials with low stiffness. The cobalt-chromium-molybdenum is about ten times stiffer than bone and the alumina is about nineteen times stiffer than bone.<sup>5</sup> The stiffness can be a problem, associated with the stress shielding,

related to the difference between the bone stiffness and implant material. Titanium alloy has low modulus of elasticity as compared with the previous materials.<sup>5</sup> New metallic alloy materials, like titanium alloys with low Young modulus are referred by different authors as promise in different applications.<sup>6,7</sup> Decreasing the implant material stiffness, would be expected an increase on the transferred load from the implant to the bone, hence decreasing the stress shielding.<sup>5</sup>

Many publications present numerical and experimental simulations used to test different femoral components combined with different shapes and materials.<sup>4,8,10</sup> Other developed works show the importance in study microelectromechanical systems and living organisms that help the scientific communities to understand the mechanics and biological structures. For this reason, carbon nanotubes, classified as microtubule-stabilizing agents, hold a substantial promising application in cancer therapy in conjunction with other cancer treatments.<sup>11</sup> Relevant studies showed a size-dependent model for the stability analysis of carbon nanotubes stabilized microtubules under radial and axial loads.<sup>11</sup> Other research showed a detailed parametric study conducted to investigate the effects of the elastic constants of surrounding medium and internal filament matrix of piezoelectric nanoshell and temperature change on the smart control of microtubules.<sup>12</sup> All of these findings and conclusions have great significance in

\* Elza M. M. Fonseca; [elz@isep.ipp.pt](mailto:elz@isep.ipp.pt)

biomechanical behavior on the transferred load to the bone and always will give more information about the better performance, dependent of the chosen material and implant size.

The implant success depends on the manner in which loads are transferred to the surrounding bone<sup>13</sup> and leads to decrease the stress shielding effect. Also, all the contribution to reduce the bone resorption, which is the process by which the bones are absorbed and broken down by the body, should be investigated according the need transferred load to the bone. Stress shielding in bone occurs when some of the loads are taken by implant and protected from going to the bone.<sup>9</sup>

Our work gives additional information about the developed stresses and transferred loads to the bone using lesser expensive computational models (two dimensional (2D) axisymmetric planes). The finite element analysis was carried out to calculate the von Mises stress, the shear stress and the strain energy density in all studied models. A simplified equation is used to compare the effect between cemented and uncemented femoral components with an implant core variable stiffness. Three different implant diameters were chosen and two materials considered, a typical titanium alloy and iso-elastic titanium alloy with low stiffness.

The goal of this work is to enlarge the knowledge of the cemented and uncemented femoral components, increasing the results with numerical models, where the authors of this study have different investigations.<sup>8,14,15</sup> It is intended to increase studied works among authors, with all type of results that a computational model can showing, and adding the study with an implant with core variable stiffness.

According this purpose, the main objectives were as follow:

- Study the load transferred to the bone in all models, implant-cement-bone (Model 1), implant-bone (Model 2) and core implant-bone (Model 3).

- Study the stress and strain at radial length, from internal to the lateral bone side, in all models.

- Study stress at bone length interface, since proximal end to distal end, in all models.

## 2. Materials and methods

2D axisymmetric computational models of an implant-cement-bone (Model 1), implant-bone (Model 2) and core implant-bone (Model 3) were constructed using the finite element method with ANSYS program. The numerical model is structural and linear, using 2D axisymmetric plane elements with 8 nodes, PLANE183.

The finite element analysis was assumed a state of ideal osseointegration, where cortical, cement and implant were assumed to be perfectly bonded. Figure 1 shows all 2D computational models in study and the respectively used mesh. Mesh convergence tests were carried out to minimize the computational error. A regular mesh was considered with a size finite element equal to 1 mm. Both models have the same regular mesh to allow the better comparison.

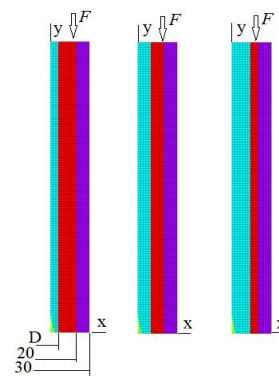
All materials were assumed linear elastic, homogeneous and isotropic. The corresponding elastic properties such as Young's modulus ( $E$ ) and Poisson ratio ( $\nu$ ) were determined from the literature.<sup>9</sup> The model consists of a homogeneous cortical bone ( $E_b=20\text{GPa}$ ), cement bone ( $E_c=2\text{GPa}$ ), titanium alloy ( $E_i=115\text{GPa}$ ) and iso-elastic titanium alloy ( $E_i=40\text{GPa}$ ) with Poisson of 0.3. The implant material is titanium alloy or iso-elastic titanium (Ti alloy (ISO)), respectively for

Model 1 and 2. In the Model 3, a vertical functionally graded combination between the two materials was considered.

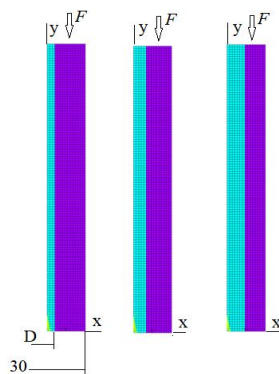
In all models, the bottom edge on Y-axis was assumed to be fixed. An average compression applied load of  $F=700\text{N}$  was determined from the literature and imposed in the model head.<sup>9</sup> The outside diameter of the bone is equal to  $d_b=30\text{mm}$  and a solid implant diameter  $D$  vary between 6, 10 and 14mm. In cemented femoral component (Model 1) the cement diameter is equal to  $d_c=20\text{mm}$ . In the Model 3 the dimensions are equal to Model 2, where the implant assumes two different materials, as a vertical graded material (D1 and D2).

The finite element analysis was carried out to calculate the von Mises stress, the shear stress and the strain energy density in all studied models, produced by the compressive load and the effect of implant material and diameter.

Model 1  
(Implant  $D=6, 10, 14$ ); Cement  $d_c=20$ ; Bone  $d_b=30$ )



Model 2  
(Implant  $D=6, 10, 14$ ); Bone  $d_b=30$ )



Model 3  
(Implant  $D=6, 10, 14$ ); Bone  $d_b=30$ )

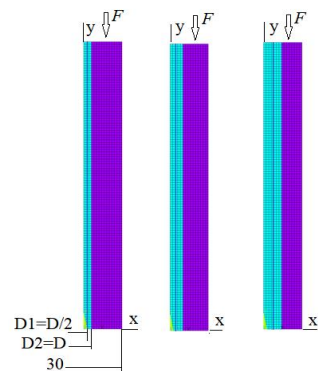


Figure 1. Different models in study.

**Table 1.** Load transferred to the bone, function of implant diameter and material

Implant diameter D, mm	Model 1, M1 D, dc=20, db=30		Model 2, M2 D, db=30		Model 3, M3 D1=D/2, D2=D, db=30	
	titanium-cement-bone	Ti alloy (ISO)-cement-bone	titanium-bone	Ti alloy (ISO)-bone	core titanium-Ti alloy (ISO)-bone	core Ti alloy (ISO)-titanium-bone
	Fbone/F	Fbone/F	Fbone/F	Fbone/F	Fbone/F	Fbone/F
6	0.6726	0.8218	0.8067	<b>0.9231</b>	<b>0.8910</b>	0.8330
10	0.4525	0.6849	0.5818	0.8000	0.7314	0.6244
14	<b>0.3035</b>	0.5480	0.3845	0.6423	0.5501	0.4274

**3. Results and discussion**

*3.1. Load transferred to the bone obtained with elastic stress theory*

A simplified equation (1), based on the elastic stress theory applied to composite materials for an axial load, should be used to measure the load transferred to the bone.

$$\frac{F_b}{F} = \frac{A_b E_b}{A_i E_i + A_c E_c + A_b E_b} \tag{1}$$

$F_b$  is the internal load transferred to the bone,  $F$  is the applied force,  $E$  is Young's modulus and  $A$  the cross-section area. Symbol  $i$  for material implant,  $b$  for bone, and  $c$  for cement (Model 1) or material implant D2 (Model 3) or  $c$  equal to zero (in Model 2). All produced results according this equation are represented in table 1 or figure 2.

A comparison between all models, it was demonstrated that material with lower stiffness increases load transferred to the bone, generating less bone resorption, with more relevance in the Model 2 (uncemented) when compared with the Model 1 (cemented implant).

Consequently, to increase the load transferred to the bone, lesser solid implant diameter with lower stiff material could be the chosen option, as Model 2 with iso-elastic titanium (Ti alloy (ISO)) and dimeter D=6.

Using the Model 3, with the vertical graded material it is found that when the material is iso-elastic titanium (Ti alloy (ISO)), neighbored to the bone and lower implant diameter the load transferred to the bone also increases, when compared with the material in titanium, neighbored to the bone.

Comparing all models, the lesser implant diameter D=6 solution with the iso-elastic titanium (Ti alloy (ISO)) vicinity to the bone (Model 2 or 3) produces the most load transferred to the bone. The worst situation is the higher implant diameter D=14 solution with the titanium alloy (Model 1).

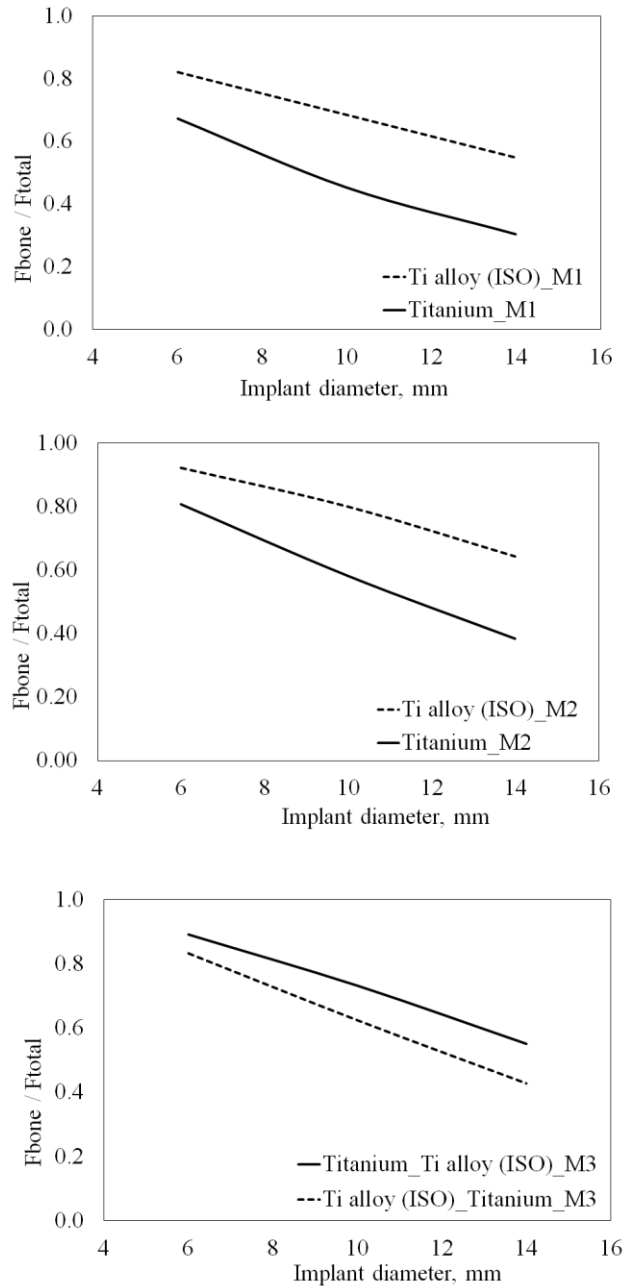


**Figure 2.** Load transferred to the bone (Models 1, 2 and 3).

**Table 2.** Comparison of results, Model 1

Implant Material	Analytical results, MPa			Numerical results, MPa			Error (%)		
	Implant	Cement	Bone	Implant	Cement	Bone	Implant	Cement	Bone
Model 1									
Titanium_D6	6.8937	0.1199	1.1989	7.0891	0.1205	1.1846	2.834	0.508	1.193
Ti alloy (ISO)_D6	2.9299	0.1465	1.4649	3.0871	0.1491	1.4520	5.366	1.793	0.883
Titanium_D10	4.6378	0.0807	0.8066	4.6036	0.0807	0.8133	0.738	0.035	0.837
Ti alloy (ISO)_D10	2.4418	0.1221	1.2209	2.5175	0.1232	1.2054	3.099	0.916	1.271
Titanium_D14	3.1108	0.0541	0.5410	3.0827	0.0543	0.5517	0.904	0.308	1.982
Ti alloy (ISO)_D14	1.9537	0.0977	0.9768	1.9751	0.0985	0.9686	1.097	0.809	0.839

**Table 3.** Comparison of results, Model 2

Implant Material	Analytical results, MPa		Numerical results, MPa		Error (%)	
	Implant	Bone	Implant	Bone	Implant	Bone
Model 2						
Titanium_D6	4.7851	0.8322	4.7867	0.8321	0.034	0.008
Ti alloy (ISO)_D6	1.9044	0.9522	1.9044	0.9522	0.001	0.000
Titanium_D10	3.7271	0.6482	3.7272	0.6482	0.002	0.001
Ti alloy (ISO)_D10	1.7825	0.8913	1.7826	0.8913	0.004	0.001
Titanium_D14	2.7989	0.4868	2.7987	0.4868	0.007	0.009
Ti alloy (ISO)_D14	1.6264	0.8132	1.6264	0.8132	0.000	0.000

**Table 4.** Comparison of results, Model 3

Implant Material	Analytical results, MPa			Numerical results, MPa			Error (%)		
	Implant D1	Implant D2	Bone	Implant D1	Implant D2	Bone	Implant D1	Implant D2	Bone
Model 3									
Titanium_Ti alloy (ISO)_D1=3, D2=6	5.2846	1.8381	0.9191	5.2855	1.8384	0.9191	0.016	0.014	0.002
Ti alloy (ISO)_Titanium_D1=3, D2=6	1.7185	4.9407	0.8593	1.7192	4.9426	0.8592	0.040	0.038	0.008
Titanium_Ti alloy (ISO)_D1=5, D2=10	4.6855	1.6297	0.8149	4.6867	1.6301	0.8148	0.025	0.022	0.009
Ti alloy (ISO)_Titanium_D1=5, D2=10	1.3912	3.9998	0.6956	1.3915	4.0006	0.6955	0.018	0.019	0.012
Titanium_Ti alloy (ISO)_D1=7, D2=14	4.0045	1.3929	0.6964	4.0050	1.3930	0.6964	0.012	0.009	0.007
Ti alloy (ISO)_Titanium_D1=7, D2=14	1.0821	3.1111	0.5411	1.0821	3.1112	0.5411	0.003	0.003	0.003

3.2. Stress and strain at radial length, from internal to the lateral bone side obtained with analytical and numerical results

Based on the elastic stress theory and using Hooke’s law, the definition of stress applied to composite materials for an axial load should be calculated with equation (2).

$$\sigma_{k=i,c,b} = \frac{F E_{k=i,c,b}}{A_i E_i + A_c E_c + A_b E_b} \quad (2)$$

$F$  is the applied force,  $E$  is Young's modulus and  $A$  the cross-section area. Symbol  $i$  for material implant,  $b$  for bone, and  $c$  for cement (Model 1) or material implant D2 (Model 3) or  $c$  equal to zero (Model 2).  $\sigma_k$  is the stress calculated in the material implant, cement or bone.

Tables 2, 3 and 4 shown the stress calculation, using the equation (2) and the obtained numerical results. It is possible to compare the results in all models in study. The numerical values, as a constant value for each femoral part, agree with the analytical results. The calculated percent error, in relation to the analytical values, is low. The higher error value is lesser than 5.4%, which represents a good agreement. Due this observation, the following results are obtained from numerical simulations, which allow a global study in all models.

Figure 3 shows all numerical results about the von Mises stress, from inside implant diameter to lateral bone side.

The load transferred to the bone increases with the lesser implant diameter and the lower stiff material, this is why, the level of von Mises stress in the bone is lesser compared with other solutions. The level of von Mises stress is higher in stiff implant material and decreases if implant diameter increases. Model 1 has three different baselines due the cement effect, where the von Mises stress has lower value. In the Model 2 (uncemented implant) the stress is less, and more constant in iso-elastic titanium (Ti alloy (ISO) implant material. In the Model 3 the stress is similar to the Model 2, the difference is in the core region of the implant material. Iso-elastic titanium (Ti alloy (ISO)) implant material in vicinity of the bone and higher diameter produce the lesser von Mises stress at radial implant section.

The elastic strain energy density  $U$  represents de recoverable part of the energy per unit volume in the model, stored in the differential material element, that is half the scalar product of the stresses  $\sigma$  and the strains  $\varepsilon$ . Equation (3) represents the strain energy density.

$$U = \frac{1}{2} \sigma \varepsilon \quad (3)$$

Figure 4 shows the values of the strain energy density in the studied models, at radial length, from internal implant diameter to the lateral bone side. The level of a bone strain is relating to the stimulus which leads to the bone remodeling.<sup>16</sup>

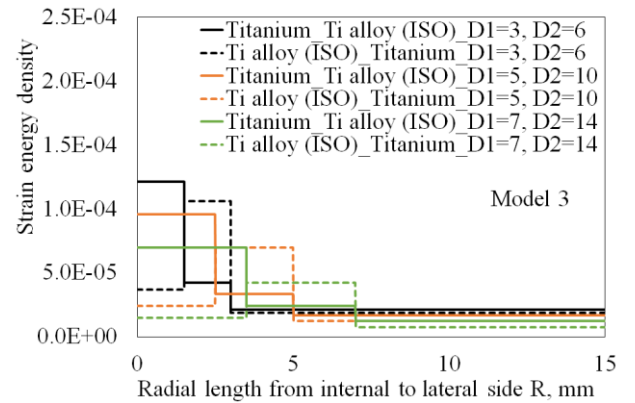
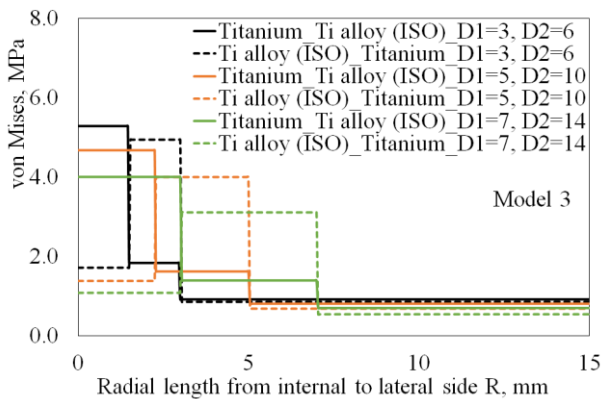
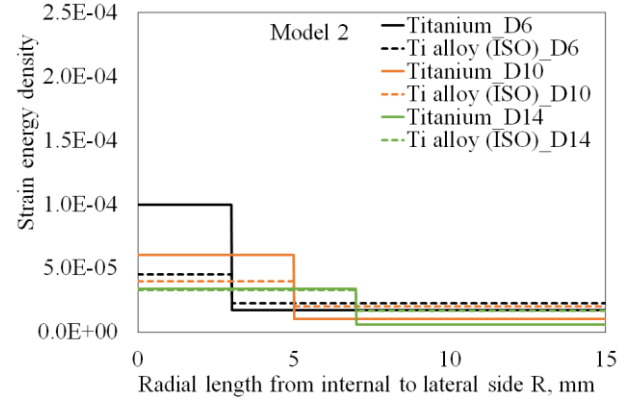
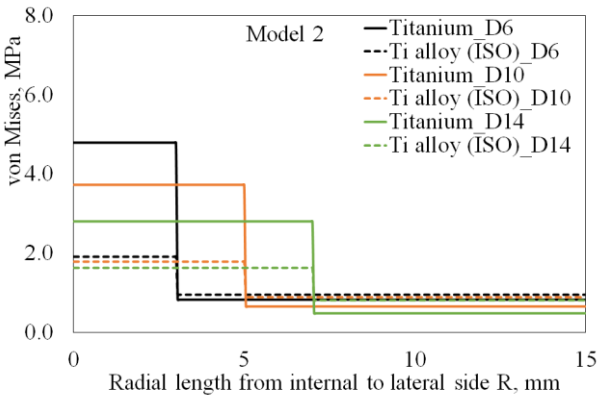
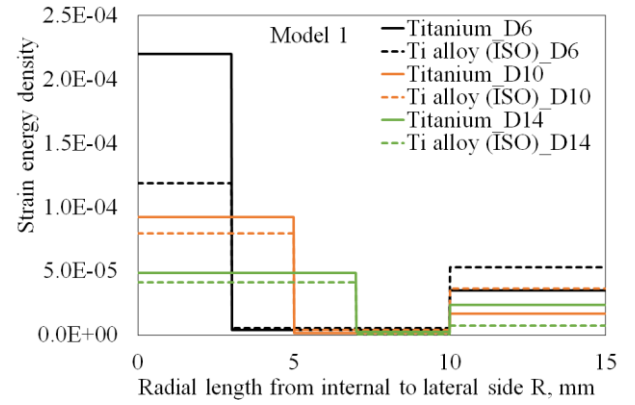
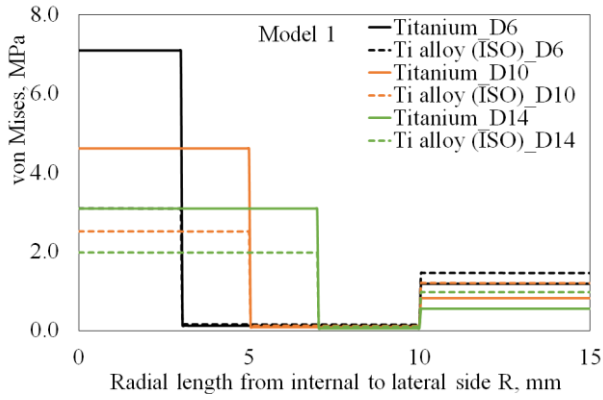


Figure 3. von Mises stress (Models 1, 2 and 3).

Figure 4. Elastic strain energy density (Models 1, 2 and 3).

The numerical results of the distribution of the strain-energy density in all models shown that, the most flexible implant material is the Model 2 (uncemented) and the most rigid implant material is Model 1 (cemented). The lesser diameter and titanium material implant exhibited higher strain energy density than that of the iso-elastic titanium (Ti alloy (ISO)) implant material. High concentration of the strain energy density may cause damage and subsequent bone absorption around the implant. It is clearly observed that the strain energy density around the implant was dramatically reduced by the cement (Model 1). Nevertheless, this fact, in the bone region the strain energy increases when comparing Model 1 with Model 2. Model 3 has a similar behavior with Model 2. All the conclusions for the elastic strain energy are very close to the previously mentioned for the von Mises stress.

Figure 5 shows the numerical results of the shear stress at radial length, from internal implant diameter to the lateral bone side.

About shear stress, the results could represent the interaction effect in the implant material interface. The maximum shear stress for both models are concentrated between the implant to the bone interface, decreased gradually towards the lateral bone side.

Model 1 represents two peaks of stress for implant material in titanium and lesser implant diameter, similar to the iso-elastic titanium (Ti alloy (ISO)) implant material. The peaks present are near to the interface implant to bone.

In the Model 2 the level of shear stress is lower compared with the other solutions.

Model 3 represents one peak at the interface, between the implant core and the bone region. The worst value is for iso-elastic titanium (Ti alloy (ISO)) in implant core material and titanium vicinity of the bone with smaller implant diameter. For the same implant material, when diameter is higher the shear stress decreases.

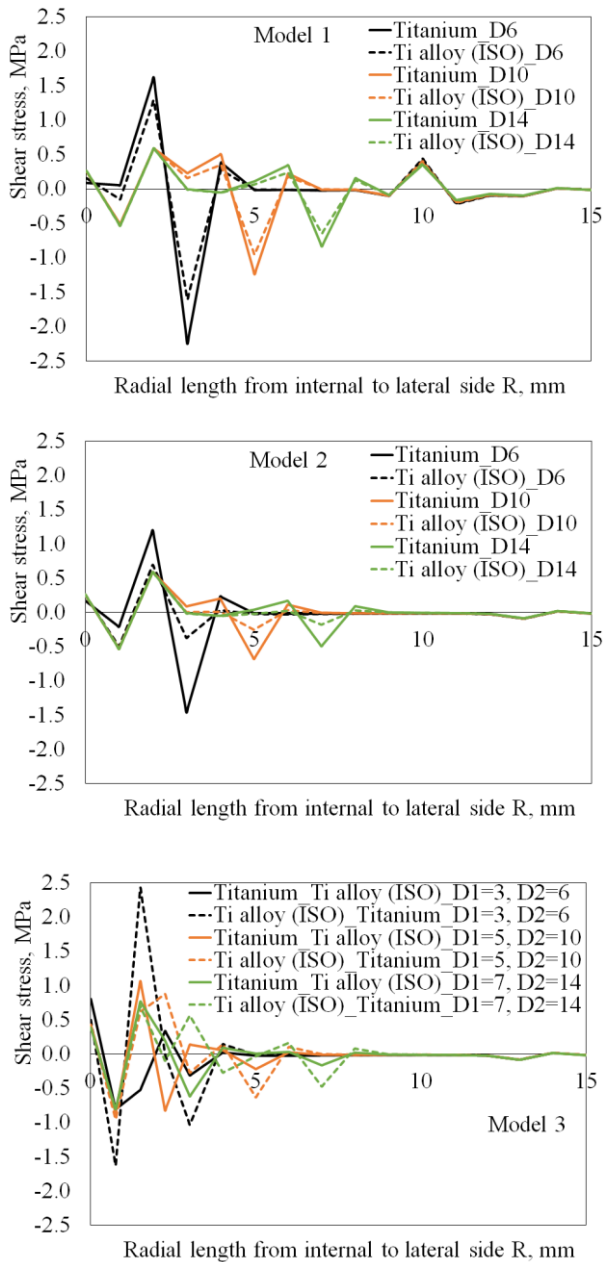


Figure 5. Shear stress (Models 1, 2 and 3).

3.3. Stress at bone length interface, since proximal end to distal end, obtained from numerical results

Figure 6 and 7 represent the von Mises and shear numerical values obtained over the bone length interface. The comparison between all models, it was demonstrated that the most von Mises or shear stress are near the proximal end and decreasing regarding the distal end, as reported by <sup>9</sup>.

It is found that the minimum von Mises stress values is occurred using cemented implant (Model 1). However, the values of von Mises stress at the bone length interface are increased using Model 2 (uncemented implant). Model 2 with small implant diameter and high stiff material produce high von Mises stress level. In the Model 3, the level of von Mises stress is high, where the lower and constant stress is obtained using material titanium in implant core and the higher implant diameter.

As a result, flexible implant produces less stress level, therefore less stress shielding in the bone, as reported by <sup>10</sup>.

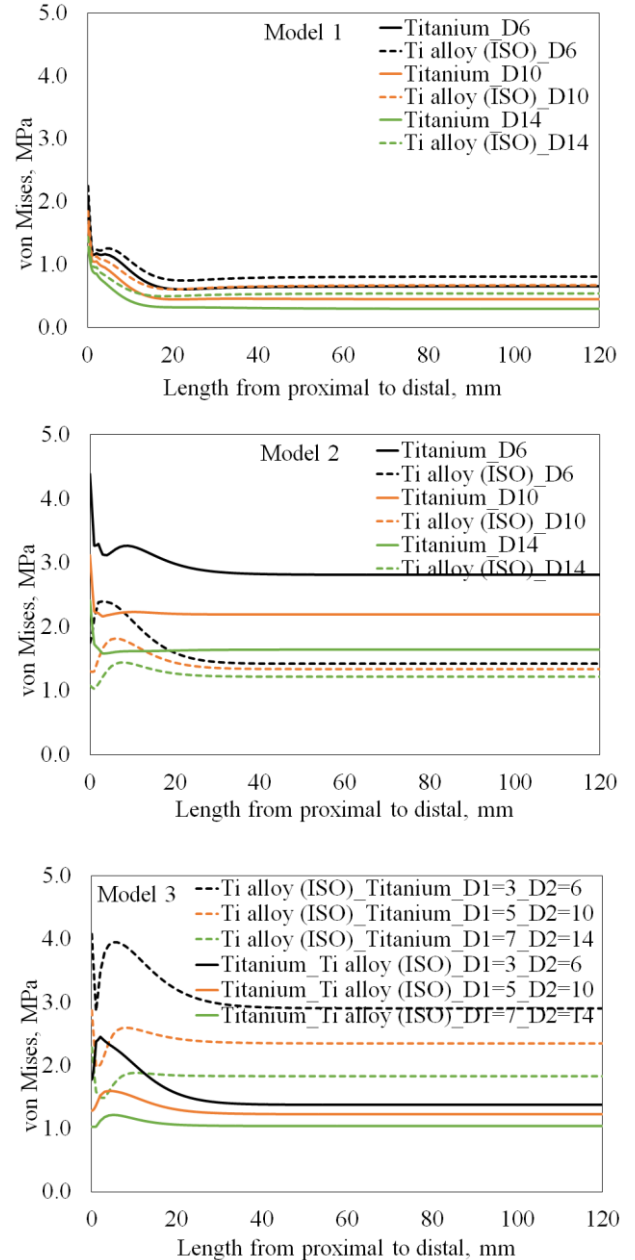


Figure 6. von Mises (MPa) at bone length interface (Models 1, 2 and 3).

One problem with flexible implant is the enhancement of relative interface motions when implant is uncemented.<sup>13</sup> Nevertheless, it is important to combine the effect with interface shear stress. Shear stress is found at the bone interface and with high effect localized proximally, as reported by other authors.<sup>13</sup> Shear stress presents a high risk for failure at the interface.

In the Model 1, due the cement effect, the peak of shear stress is very similar between materials and used implant diameters, and lesser when compared with the other models.

Model 2 represents localized high shear stress, at proximal end, where the influence of stiffer material and lesser implant diameter allow the most critical peak. Iso-elastic titanium and the combination with higher implant diameter allow lesser shear stress.

Model 3 represents lesser shear stress in comparison with the Model 2, when the vertical graded has Ti alloy (ISO) vicinity to the bone and higher implant diameter.

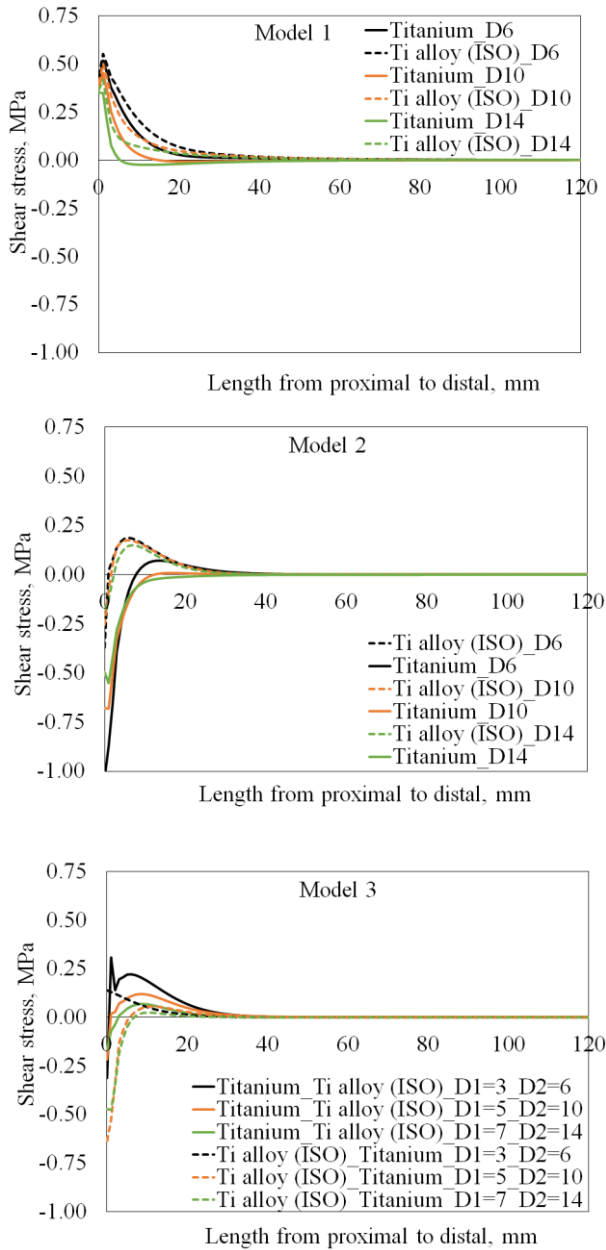


Figure 7. Shear stress (MPa) at bone length interface (Models 1, 2 and 3).

According to the research from<sup>17</sup>, increasing cement thickness, tensile stress is reduced by fifty percent and shear stress at least twelve percent.

This type of observation was verified in our models, when the same implant (diameter and material) was used in the Models 1 and 2.

The level of stress is more reduced always in Model 1. Model 3 (core titanium-Ti alloy (ISO)-bone) is an alternative to produce lower stress level with the higher implant diameter.

4. Limitation

There are some points to discuss the limitation of our study. The major limitation is that some of our data were based on published articles, where our femoral component was assumed as specific for our study.

Our studied femoral component, as a numerical model, may not reproduce the similar condition in another model. The use of patient geometry is mandatory for a thorough clinical clarification. The bone mechanical properties were assumed to be isotropic, independent of gender and age, and only the cortical part was included.

Nevertheless, the studied model produced relevant conclusions that it is important to give attention, where the materials combinations played a significant importance. In future studies, based in previous, the cortical and cancellous bone should be considered, as orthotropic material. This drawback seems unavoidable to extend our contribution.

5. General conclusions

The maximum stresses occur at or very near the implant cement interface, indicating the probability of debonding, as an initialing mechanism in the implant loosening process.<sup>17</sup>

The level of shear stresses is in the same range as the von Mises stress, whereby it is important to consider due the probable failure models.

Flexible implants reduce stress shielding and bone resorption, however they increase interface stresses<sup>10</sup>, as the previous obtained results.

In all models, the strain energy density and von Mises stress were severely concentrated around the implant, being the concentration in the Model 1 was higher than in the Model 2 and 3, suggesting bone absorption around the implant of the Model 1.

About the proposed Model 3, in all results, the vertical graded Ti alloy (ISO) in vicinity to the bone with high diameter has a good performance, figure 8.

Also, lesser implant diameter and the iso-elastic titanium (Ti alloy (ISO)) material, vicinity to the bone (Model 2 or Model 3), produce the most load transferred to the bone. Nevertheless, Models 2 and 1 have a behavior, that were possible to obtain good solutions.

Figure 8 shows the numerical results obtained for the Model 3 (core titanium-Ti alloy (ISO)-bone; D=14), using the 2D axisymmetric plane element, which it allowed possible to generate a 3D solid of revolution, to analyze the previous discussed. .

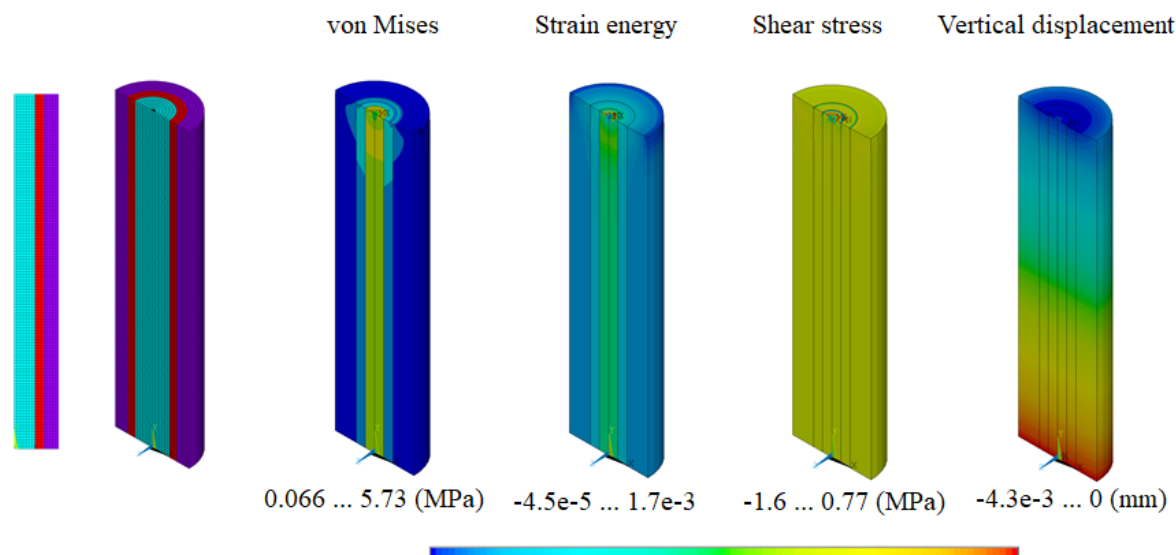


**Figure 8.** Numerical results of the Model 3 (core titanium-Ti alloy (ISO)-bone; D=14).

## References

- [1] Chia-Ching Lee, Shang-Chih Lin, Ming-Jen Kang, Shu-Wei Wu, Ping-Yuen Fu, 2010, Effects of implant threads on the contact area and stress distribution of marginal bone, *J Dent Sci*, doi:10.1016/S1991-7902(10)60023-2
- [2] VK Ganesh, K Ramakrishna, Dhanjoo N Ghista, 2005, Biomechanics of bone-fracture fixation by stiffness-graded plates in comparison with stainless-steel plates, *BioMedical Engineering OnLine*, doi:10.1186/1475-925X-4-46
- [3] Harrie Weinans, Rik Huiskes and Henk J. Grootenboer, 1992, Effects of Material Properties of Femoral Hip components on Bone Remodeling, *Journal of Orthopaedic Research*, doi:10.1002/jor.1100100614
- [4] Kristina Haase, Gholamreza Rouhi, 2013, Prediction of stress shielding around an orthopedic screw: Using stress and strain energy density as mechanical stimuli, *Computers in Biology and Medicine*, doi:10.1016/j.combiomed.2013.07.032
- [5] M.I.Z. Ridzwan, Solehuddin Shuib, A.Y. Hassan, A.A. Shokri and M.N. Mohamad Ibrahim, 2007, Problem of Stress Shielding and Improvement to the Hip Implant Designs: A Review, *J. Med. Sci.*, doi:10.3923/jms.2007.460.467
- [6] N. Fouda, 2014, Horizontal Functionally Graded Material Coating of Cementless Hip Prosthesis, *Trends Biomater. Artif. Organs*, 28(2): 58-64.
- [7] U. Simon, P. Augat, A. Ignatius, L. Claes, 2003, Influence of the stiffness of bone defect implants on the mechanical conditions at the interface - a finite element analysis with contact, *Journal of Biomechanics*, doi:10.1016/s0021-9290(03)00114-3
- [8] M.G. Fernandes, J.L. Alves, E.M.M. Fonseca, 2016, Diaphyseal femoral fracture: 3D biomodel and intramedullary nail created by additive manufacturing, *International Journal of Materials Engineering Innovation*, doi:10.1504/IJMATEL.2016.079556
- [9] M.I.Z. Ridzwan, Solehuddin Shuib, A.Y. Hassan, A.A. Shokri, 2006, Effects of Increasing Load Transferred in Femur to the Bone-Implant Interface, *Journal of Applied Sciences*, doi:10.3923/jas.2006.183.189
- [10] Rik Huiskes. 1993, Failed innovation in total hip replacement. Diagnosis and proposals for a cure, *Acta Orthop Scand*, doi:10.3109/17453679308994602
- [11] E. Rohani Rad, M.R. Farajpour, 2019, Influence of taxol and CNTs on the stability analysis of protein microtubules, doi:10.22059/jcmech.2019.277874.369
- [12] A. Farajpour, A. Rastgoo, M. Mohammadi, 2017, Vibration, buckling and smart control of microtubules using piezoelectric nanoshells under electric voltage in thermal environment, *Physica B: Condensed Matter*, doi:10.1016/j.physb.2017.01.006
- [13] Toufik Bousnane, Smail Benbarek, Abderahmen Sahli, Boualem Serier, Bel Abbes Bachir Bouiadjra, 2018, Damage of the Bone-Cement Interface in Finite Element Analyses of Cemented Orthopaedic Implants, *Periodica Polytechnica Mechanical Engineering*, doi:10.3311/PPme.11851
- [14] Maria G. Fernandes, Elza M. Fonseca, Renato N. Natal; 2019, Thermo-mechanical stresses distribution on bone drilling: numerical and experimental procedures, *Proceedings of the Institution of Mechanical Engineers, Part L: Journal of Materials: Design and Applications*, doi:10.1177/1464420716689337
- [15] E.M.M.Fonseca, M.J.Lima, L.M.S.Barreira, 2009, Human femur assessment using isotropic and orthotropic materials dependent of bone density, *Third International Conference on Integrity, Reliability & Failure*, S. Gomes et al (Eds.), Edições INEGI, Proceedings IRF'2009, paper Ref: S1904\_P0345.
- [16] Raouf Korabi, Keren Shemtov-Yona, DDS, Daniel Rittel, 2017, On stress/strain shielding and the material stiffness paradigm for dental implants, *Clin Implant Dent Relat Res*. doi:10.1111/cid.12509
- [17] I.Y. Lee, M.D., H.B. Skinner, M.D., J.H. Keyak, M.D., 1993, Effects of Variation of Cement Thickness on Bone and Cement Stress at the Tip of a Femoral Implant, *The Iowa Orthopaedic Journal*, 13: 155-159.